Cellular Oncology 32 (2010) 285–300
DOI 10.3233/CLO-2010-0511
IOS Press

The pan-deacetylase inhibitor panobinostat inhibits growth of hepatocellular carcinoma models by alternative pathways of apoptosis

Pietro Di Fazio [a,b,h,*], Regine Schneider-Stock [c,*], Daniel Neureiter [d], Kinya Okamoto [a,e], Till Wissniowski [a], Susanne Gahr [a], Karl Quint [a,h], Matthias Meissnitzer [d], Beate Alinger [d], Roberta Montalbano [b,h], Gabriele Sass [f], Bernd Hohenstein [g], Eckhart G. Hahn [a] and Matthias Ocker [a,h,**]

[a] *Department of Medicine 1, University Hospital Erlangen, Erlangen, Germany*
[b] *Dipartimento di Scienze Biochimiche, Universita di Palermo, Policlinico, Palermo, Italy*
[c] *Department of Pathology, University Hospital Erlangen, Erlangen, Germany*
[d] *Institute of Pathology, Salzburger Landeskliniken, Paracelsus Private Medical University, Salzburg, Austria*
[e] *Second Department of Internal Medicine, Tottori University School of Medicine, Tottori, Japan*
[f] *Division of Experimental Immunology and Hepatology, University Medical Center Hamburg Eppendorf, Hamburg, Germany*
[g] *Department of Medicine 4, University Hospital Erlangen, Erlangen, Germany*
[h] *Institute for Surgical Research, Philipps-University Marburg, Marburg, Germany*

Abstract. Inhibition of deacetylases represents a new treatment option for human cancer diseases. We applied the novel and potent pan-deacetylase inhibitor panobinostat (LBH589) to human hepatocellular carcinoma models and investigated by which pathways tumor cell survival is influenced.

HepG2 (p53wt) and Hep3B (p53null) responded to panobinostat treatment with a reduction of cell proliferation and a significant increase in apoptotic cell death at low micromolar concentrations. Apoptosis was neither mediated by the extrinsic nor the intrinsic pathway but quantitative RT-PCR showed an upregulation of CHOP, a marker of the unfolded protein response and endoplasmic reticulum stress with subsequent activation of caspase 12. Dependent on the p53 status, a transcriptional upregulation of $p21^{cip1/waf1}$, an increased phosphorylation of H2AX, and an activation of the MAPK pathway were observed. In a subcutaneous xenograft model, daily i.p. injections of 10 mg/kg panobinostat lead to a significant growth delay with prolonged overall survival, mediated by reduced tumor cell proliferation, increased apoptosis and reduced angiogenesis in tumor xenografts. Panobinostat increased the acetylation of histones H3 and H4.

Panobinostat is a well tolerated new treatment option for HCC that activates alternative pathways of apoptosis, also in p53-deficient tumors.

Keywords: $p21^{cip1/waf1}$, unfolded protein response (UPR), endoplasmic reticulum stress, caspase 12, transcriptional regulation, xenograft model, HDAC, LBH589

1. Introduction

Hepatocellular carcinoma (HCC) represents an unmet medical need. It is the fifth most common malignancy worldwide and shows rising incidences in Western countries [11]. Usually developing on the basis of advanced cirrhosis, treatment options still remain limited and are of palliative character [30,39].

Recently, inhibitors of protein deacetylases (DACi) and histone deacetylases (HDACi) have been established as potent novel anti-cancer therapeutics [38, 43]. Several compounds have been developed on the basis of hydroxamic acid derivates and vorinostat

[*] The first two authors contributed equally to this work.

[**] Corresponding author: Prof. Dr. Matthias Ocker, MD, Institute for Surgical Research, Baldingerstrasse, 35043 Marburg, Germany. Tel.: +49 6421 5868930; Fax: +49 6421 5868926; E-mail: Matthias.Ocker@staff.uni-marburg.de.

(suberoylanilide hydroxamic acid) has recently been approved for clinical use against cutaneous T-cell lymphomas [9]. Various hydroxamic acid derivatives have also been applied to human HCC models and demonstrated specific pro-apoptotic effects and to sensitize HCC cells to conventional or novel targeted chemotherapeutic agents [12,18,28,32].

Inhibition of HDACs leads to the re-expression of epigenetically silenced genes like the tumor suppressor $p21^{cip1/waf1}$ or the TRAIL death receptor system [5,29,32]. This effect is usually attributed to a p53-dependent reactivation of transcription but further effects independent of a transcriptional control and modifications of non-histone proteins have been described [43].

The novel cinnamic hydroxamic acid pan-DACi panobinostat (LBH589) has recently been described to possess cytotoxic properties against different human cancer cell lines and to human cancer xenografts in nude mice [10,23,34]. Panobinostat has also demonstrated a good tolerability in a phase I study in humans with refractory hematologic malignancies [15].

We therefore applied panobinostat to human HCC cell lines *in vitro* and to a xenograft model *in vivo* to determine its efficacy and molecular pathways as an anti-cancer agent for the treatment of HCC.

2. Materials and methods

2.1. Cell culture

The human hepatoma cell lines HepG2 (p53wt) and Hep3B (p53null) as well as primary human foreskin fibroblasts (HF, p53wt) were cultured under standard conditions as described previously [28]. HF served as a non-malignant epithelial control cell line for toxicity screening (cell viability and apoptosis rate) as primary human hepatocytes are unstable under cell culture conditions. For all *in vitro* experiments, 150,000 cells were seeded to 6-well tissue culture plates 24 h before treatment. Cells were treated with panobinostat at 0.01–10 μM and analyzed or processed for further experiments after 6–120 h. Panobinostat (LBH589) was provided by Novartis Pharma AG (Basel, Switzerland) and prepared as previously described [34].

2.2. Analysis of cell viability and apoptosis

Proliferation rate was determined by counting the number of viable cells after Trypan blue staining in a Neubauer chamber. Cell numbers were then expressed relative to untreated controls set at 1.0. Flow cytometry was employed for the quantification of apoptosis in treated cell lines after staining with propidium iodide as described previously [28]. Analysis of labeled nuclei was performed on a FACSCalibur flow cytometer (FACS) using CELLQuest software (both from Becton Dickinson). The percentage of apoptotic cells was determined by measuring the fraction of nuclei with a sub-diploid DNA content. Ten thousand events were collected for each sample analyzed. To block death receptor signaling, cells were incubated for 48 h together with 0.1 μM panobinostat with specific antibodies blocking either hDR4 (TRAIL-R1) or hDR5 (TRAIL-R2), both from Axxora Deutschland GmbH, Lörrach, Germany, at a concentration of 10 μg/ml. Recombinant human TRAIL (rhTRAIL, Alexis Biochemicals, Lörrach, Germany) was used to stimulate the extrinsic apoptosis pathway at 1 μg/ml. To inhibit caspase activity, cells were treated with the pan-caspase inhibitor z-VAD (R&D Systems, Wiesbaden, Germany) or the caspase 12 inhibitor ATAD (BioVision, Mountain View, CA, USA) at 100 μM together with 0.1 μM panobinostat for 48 h.

2.3. Xenograft model of hepatocellular carcinoma

HepG2 cell lines were harvested and resuspended in sterile physiologic NaCl solution. 5.0×10^6 cells were injected subcutaneously into the flank of 6–8 week old male NMRI mice (Harlan Winkelmann GmbH, Germany). Eight animals were used for each treatment group. Animals were kept in a light- and temperature-controlled environment and provided with food and water *ad libitum*. Tumor size was determined daily by measurement using a caliper square. When subcutaneous tumors reached a diameter of 7 mm, daily i.p. treatment with panobinostat (10 mg/kg) or vehicle (physiologic saline solution) was started. Animals were sacrificed by cervical dislocation and tumor samples collected when reaching the termination criteria (e.g., weight loss $> 20\%$, tumor diameter > 25 mm or tumor ulceration through the skin) or after 30 days of treatment. Tumor and tissue samples were fixed in 10% phosphate-buffered formalin or snap-frozen in liquid nitrogen. Blood samples were obtained before beginning of treatment and at the study endpoint. Alanine amino transferase (ALT) levels were determined using an automated procedure on a Cobas Mira (Roche, Mannheim, Germany). All animals received humane care. The study protocol complied with the institute's

guidelines and was approved by the Government of Lower Franconia (Würzburg, Germany, file number 54-2531.31-3/06) before the beginning of the experiments. Hep3B cells proved not to be tumorigenic in NMRI mice and were therefore not used for *in vivo* experiments.

2.4. Quantitative real time RT-PCR

For quantitative real time PCR, total cellular RNA was extracted by use of peqGOLD RNA Pure (Peqlab, Erlangen, Germany) according to the manufacturer's instructions and reverse transcription (RT) was performed as described previously [27]. QuantiTect Primers were purchased from Qiagen (Hilden, Germany) and run with the LightCycler FastStart DNA Master SYBR Green I kit (Roche Molecular Biochemicals, Mannheim, Germany) on a LightCycler System (Roche). Results were analyzed with the LightCycler software and normalized to GAPDH mRNA content for each sample.

2.5. Protein extraction and western blot analysis

Whole cell lysates were prepared from both cell lines with or without treatment of panobinostat. Protein preparation and immunoblotting was performed as described previously [16]. Briefly, the following antibodies were used: anti-p53 (Oncogene, San Diego, CA, USA), -p21WAF1 (DakoCytomation, Glostrup, Denmark), -acetyl-H3 (Lys14) and H4 (Lys12; Upstate, Lake Placid, NY, USA), -HDAC1 (Santa Cruz Biotechnology, Santa Cruz, CA, USA), -bax (DakoCytomation), -bcl-2, -p-p38, -p-JNK, -p-ERK, -caspase 3, -caspase 8, -caspase 9 (all from Cell Signaling, Carpinteria, CA, USA), -p-H2A.X (Upstate, Temecula, CA, USA), -CHOP, -eIF2α, p-eIF2α (all from Abcam, Cambridge, UK) and the secondary antibodies (anti-mouse or anti-rabbit IgG peroxidase conjugated; Pierce, Rockford, IL, USA). Bound antibodies were detected by incubating the blots in West Pico chemiluminescent substrate (Pierce). The level of immunoreactivity was then measured as peak intensity using an image capture and analysis system (GeneGnome, Syngene, UK). Hybridization with anti-β-actin (Sigma, Deisenhofen, Germany) was used to control equal loading and protein quality.

2.6. Chromatin-Immunoprecipitation (ChIP)

The ChIP assay was performed using the ChIP Assay Kit according to the manufacturer's protocol (Upstate, NY, USA) and as described previously [16]. After crosslinking, sonification and centrifugation steps, the supernatants were collected and diluted in ChIP dilution buffer. Two percent of the diluted cell supernatant was kept for DNA quantification and considered as inputs. Samples were incubated for 30 min at 4°C with salmon sperm DNA/protein A/protein G agarose 50% slurry before overnight immunoprecipitation with the appropriate antibody (anti-p53, Oncogene, San Diego, CA, USA). A portion of each sample was removed before immunoprecipitation and served as a negative control. After de-crosslinking, DNA was extracted by phenol/chloroform, precipitated with 96% ethanol and resuspended in H_2O for PCR. Sequences of primers, PCR product length, and annealing temperatures are given in [16].

2.7. Caspase activity assays

HepG2 and Hep3B cells were treated with panobinostat as described and incubated with lysis buffer solution (Biovision, Mountain View, CA, USA). Protein concentration was determined by BCA assay Kit according the manufacturer's recommendations (Pierce, Rockford, IL, USA). 50 µg of total protein were used for analysis. Caspase activity was determined with the Caspase Glo-8, the Caspase Glo-3/7 assay (both from Promega GmbH, Mannheim, Germany) or the Caspase-12 Fluorometric Assay Kit (Biovision, Mountain View, CA, USA) according the manufacturer's protocol and a Tecan GENios fluorometer (Genios, Tecan Germany GmbH, Crailsheim, Germany). All data were normalized to untreated controls.

2.8. Immunohistochemistry and TUNEL staining

Tumor specimens were processed as described previously [27]. Specimens were incubated with an anti-Ki-67 antibody (1:500; Dako Germany) to determine the proliferation rate. Endothelial staining was performed with the anti-MECA-32 antibody (1:1), produced in a rat hybridoma cell line [17]. TUNEL stainings were performed with the *In situ* Cell Death detection Kit (Roche, Mannheim, Germany) according to the manufacturer's instructions. Slides were digitized and analyzed with the ImageAccess Enterprise 5 software (Imagic Bildverarbeitung, Glatt-

brugg, Switzerland). Quantification (extensity) and semi-quantification (intensity and distribution) were performed in each slide, performed with electronic filtering for respective signals.

2.9. Statistical analysis

Statistical analysis was performed using SPSS 15.0.1 for Windows (SPSS Inc., Chicago, IL, USA). Animal survival was estimated by the Kaplan–Meier method comparing the survival curves with the log-rank test. Significance was calculated using the t-test for paired samples. $P < 0.05$ was regarded as significant.

3. Results

3.1. Panobinostat inhibits proliferation and induces apoptotic cell death in HCC cell lines

Cell viability was assessed in HepG2 and Hep3B liver cancer cell lines and in primary human foreskin fibroblasts (HF) by trypan blue staining and quantification in a Neubauer chamber. Both tumor cell lines showed a significant reduction in the number of viable cells already at sub-micromolar concentrations (Fig. 1A and C), while non-transformed HF showed only minor responses (Suppl. Fig. 1A: www.qub.ac.uk/isco/JCO/). In parallel, apoptosis induction was more pronounced in the HCC cell lines (Fig. 1B and D) than in HF (Suppl. Fig. 1B: www.qub.ac.uk/isco/JCO/). Both HCC cell lines showed a significant response in growth inhibition and apoptosis induction already at 0.1 μM panobinostat.

We therefore used this concentration for further *in vitro* experiments. Apoptosis was verified by morphologic assessment of cytokeratin 18 cleavage fragments (Suppl. Fig. 1C: www.qub.ac.uk/isco/JCO/) and by showing DNA fragmentation in flow cytometry (Suppl. Fig. 1D: www.qub.ac.uk/isco/JCO/). In HepG2 and Hep3B, a significant increase in sub-diploid events was determined after 48 h of 0.1 μM panobinostat, while HF did not respond under these conditions. FACS analyses also showed a cell cycle arrest in the G_1 phase in both responsive cell lines which can be explained by the increase of the cell cycle inhibitor $p21^{cip1/waf1}$ independent of the p53-status (see below and Fig. 3B) [29]. Western blot analysis of HCC cells (Fig. 2A) showed a time-dependent increase in active caspase 3 cleavage fragments. Densitometric analysis revealed a 3.2-fold and 2.5-fold increase compared to untreated controls in HepG2 and Hep3B, respectively, after 48 h treatment with 0.1 μM panobinostat.

3.2. Apoptosis is not mediated via classical pathways

To investigate the role of the mitochondrial pathway of apoptosis induction, western blot analysis of bax, bcl-2 (Fig. 2B) and caspase 9 was performed (Fig. 2C). Surprisingly, panobinostat treatment shifted the bax/bcl-2 ratio slightly towards survival in HepG2 cells (0.57 at 6 h and 0.44 at 48 h) with a strong increase in bcl-2 signals (2.7-fold). In parallel, no significant increase in active caspase 9 was detected. In Hep3B, neither bax nor bcl-2 were detectable and only a slight increase in active caspase 9 signals was observed. Furthermore, mitochondrial transmembrane potential $\Delta\Psi_m$ was determined by flow cytometry after $DiOC_6$ staining (Suppl. Fig. 2: www.qub.ac.uk/isco/JCO/). After 48 h of treatment, panobinostat did not lead to a breakdown of $\Delta\Psi_m$ in both HCC cell lines, corroborating the above described western blot results. We next analysed the expression and activation of caspase 8 by panobinostat (Fig. 2D). While only a 1.7-fold induction of caspase 8 was observed in HepG2, Hep3B showed a strong increase in active caspase 8 (17.5-fold) with a concomitant decrease in pro-caspase 8 (0.6-fold) indicating a strong role of the extrinsic pathway of apoptosis induction in p53-deficient HCC cell lines. To further asses the role of caspases in panobinostat-mediated cell death, cells were incubated with the pan-caspase inhibitor z-VAD before adding panobinostat. z-VAD alone did not influence cell viability, apoptosis or caspase 8 activity (data not shown). While the combination with 0.1 μM panobinostat lead to a significant reduction of both caspase 8 activity and apoptosis values (Fig. 2E and F), no effect on overall cell proliferation was observed (data not shown). As quantitative PCR (see below) also showed an increased expression of the pro-apoptotic TRAIL-receptor hDR4 in Hep3B cells (Fig. 3A), recombinant human TRAIL and inhibitory antibodies were used to investigate the extrinsic apoptosis signaling. While TRAIL alone did not affect apoptosis levels in the investigated cell lines, a synergistic effect was observed in combination with 0.1 μM panobinostat which was not affected by the additional incubation with antibodies blocking either hDR4 or hDR5 (Fig. 2G). Only the pan-caspase inhibitor z-VAD reduced the level of apoptosis in HepG2 cells in this setting. The combination of antibodies against hDR4 or hDR5 with panobinostat did not affect caspase 8 activity, cell proliferation or apoptosis levels compared to panobinostat alone (Fig. 2E–G), indicating that death receptor activation does not contribute to apoptosis induction even in p53-negative cells showing a high activity of caspase 8.

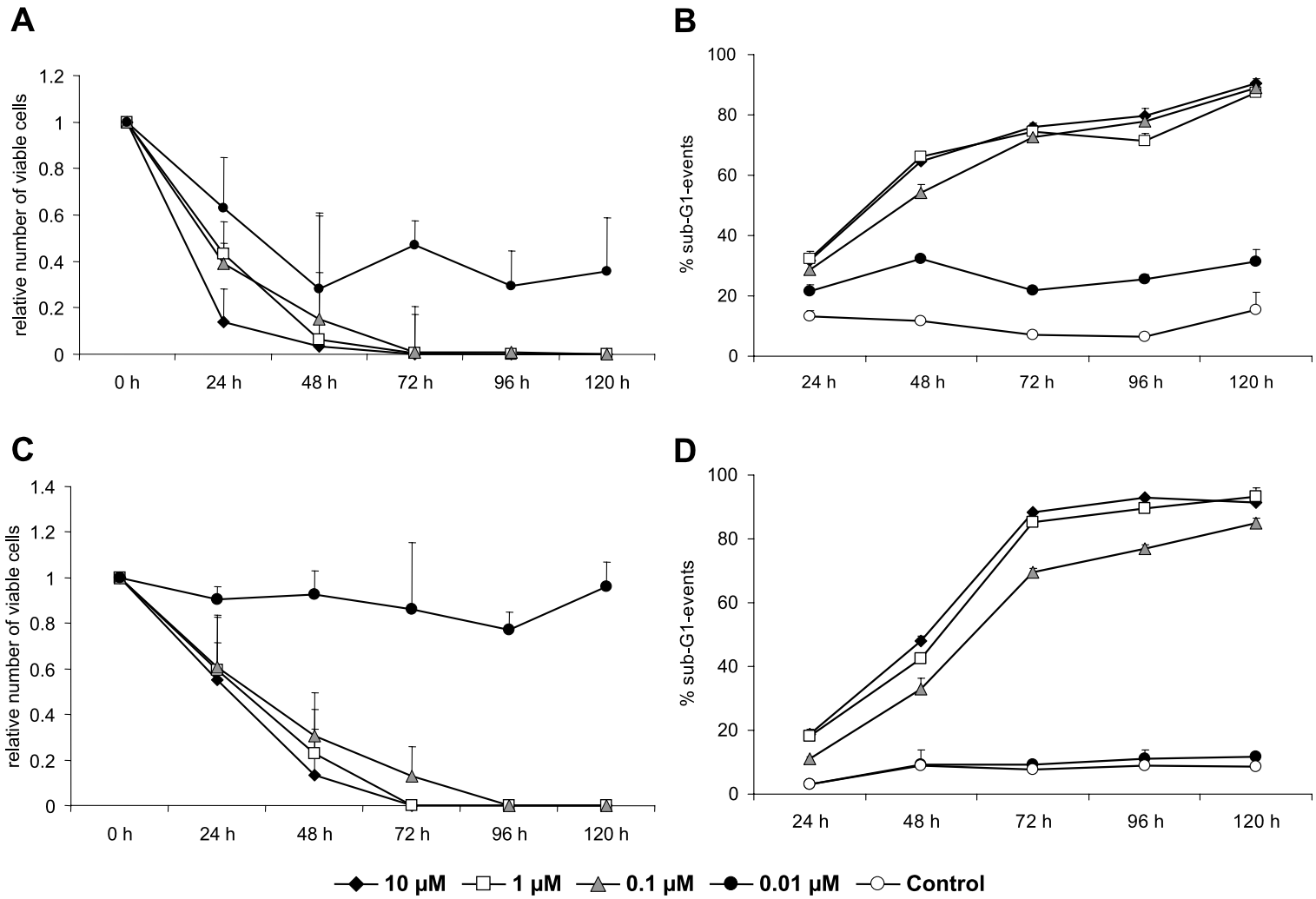

Fig. 1. Growth inhibition and induction of apoptosis in HCC cell lines by panobinostat. HepG2 (A, B) and Hep3B (C, D) were incubated with panobinostat as indicated. Proliferation (A, C) and apoptosis rate (B, D) were determined as described. Number of viable control cells was set at 1.0 in (A) and (C), other cell numbers are expressed relative to control. Shown are mean ± SEM of three independent experiments.

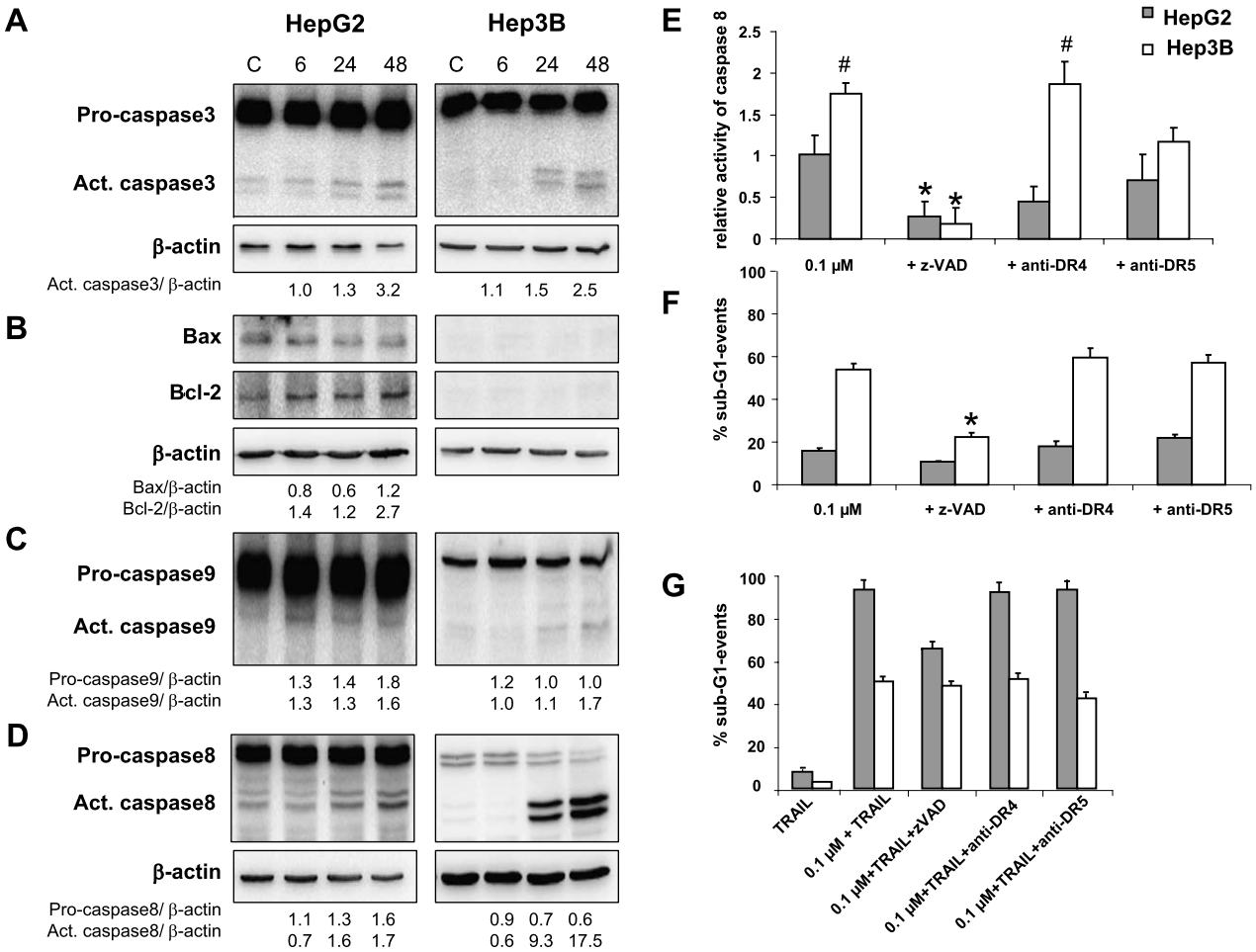

Fig. 2. Analysis of intrinsic (mitochondrial) and TRAIL-dependent (extrinsic) apoptosis pathways. Western blot analysis reveals activation of caspase 3 in both HCC cell lines after treatment with 0.1 μM panobinostat (A) but no changes in bax, bcl-2 (B) and caspase 9 (C). Analysis of expression and activation of caspase 8 after treatment with 0.1 μM panobinostat (D) shows an activation of the extrinsic apoptosis pathway in Hep3B cells. Densitometric values are normalized to β-actin and expressed relative to protein levels of untreated controls (set at 1.0). β-actin of caspase 3 also belongs to caspase 9 results. Activity of caspase 8 (E) is increased in Hep3B after incubation with panobinostat but not in HepG2. The pan-caspase inhibitor z-VAD blocks the panobinostat effect in both cell lines, while inhibitory antibodies do not influence caspase 8 activity. (F) z-VAD reduces the levels of apoptosis induced by panobinostat in Hep3B while other treatments do not interfere with HDACi. (G) Apoptosis levels after treatment with TRAIL alone or combinations of 0.1 μM panobinostat, TRAIL and specific inhibitors of caspases (zVAD) and death receptors (anti-DR4 or anti-DR5). $^{\#}P < 0.05$ vs. untreated control, $^{*}P < 0.05$ vs. 0.1 μM panobinostat. Results are mean ± SEM of three independent experiments.

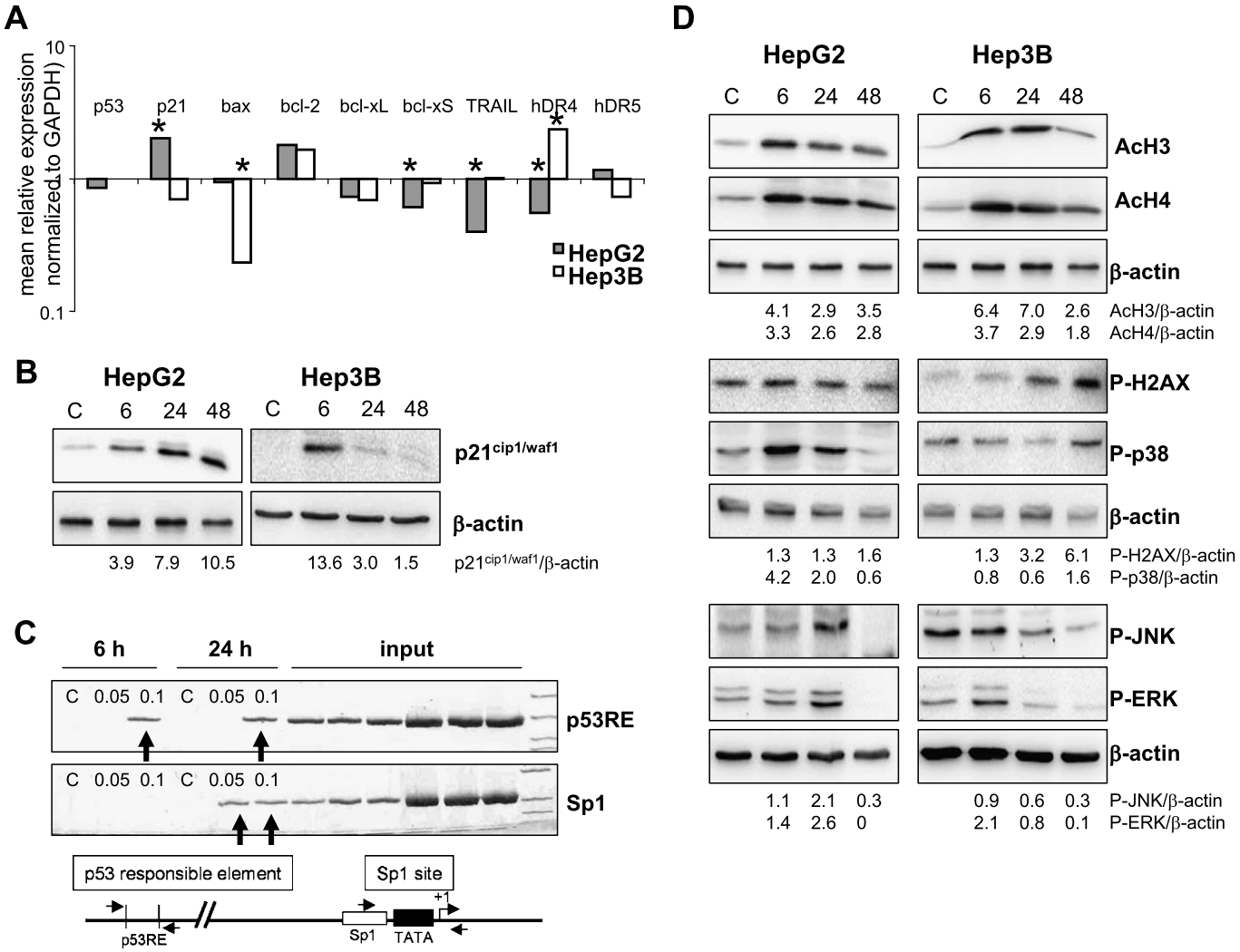

Fig. 3. Differential regulation of signal transduction pathways. (A) Quantitative *real-time* RT-PCR analysis after 48 h treatment with 0.1 μM panobinostat. mRNA expression was normalized to GAPDH and results are expressed relative to untreated controls set at 1.0. $*P < 0.05$ vs. control. p53 was not detectable in Hep3B. (B) Western blot analysis of $p21^{cip1/waf1}$ expression in HepG2 and Hep3B. (C) Chromatin immunoprecipitation (ChIP) of the $p21^{cip1/waf1}$ promoter in HepG2 cells showing a binding of the p53-responsive element (p53RE) already after 6 h and a subsequent transactivation of the Sp1 binding site after 24 h (arrows). (D) Western blot results for further signaling molecules after incubation with 0.1 μM panobinostat. Densitometry results were normalized to β-actin content and are expressed relative to untreated controls set at 1.0.

3.3. Differential regulation of signal transduction pathways

Quantitative real-time RT-PCR was performed to analyse the effect of panobinostat on expression levels of various survival and apoptosis-related genes (Fig. 3A). As expected, panobinostat induced the expression of $p21^{cip1/waf1}$ mRNA in p53-competent HepG2 cells but not in p53-deficient Hep3B after 48 h. In parallel to the western blot results described above, mRNA of pro-apoptotic bax was downregulated (significantly decreased in Hep3B) and anti-apoptotic bcl-2 was increased after 48 h of panobinostat treatment in both cell lines, thus also shifting the bax/bcl-2 ratio on the mRNA level towards survival. Anti-apoptotic Bcl-xL and pro-apoptotic bcl-xS were concomitantly downregulated in both cell lines. Analysis of the extrinsic apoptosis pathway showed a pronounced decrease of mRNA levels of TRAIL and its cognate death receptor hDR4 in HepG2 while this receptor was significantly increased in Hep3B cells. Only minor changes were observed for the TRAIL receptor hDR5.

The expression of $p21^{cip1/waf1}$ was further analysed by western blot (Fig. 3B). As expected from the mRNA results, a continuous increase of $p21^{cip1/waf1}$ was observed in HepG2 (10.5-fold after 48 h). In Hep3B, a strong, but only transient increase of $p21^{cip1/waf1}$ was observed after 6 h (13.6-fold) that decreased to control levels after 48 h (1.5-fold). As these findings indicate a p53-dependent transcriptional control of $p21^{cip1/waf1}$ expression, a chromatin immunoprecipitation (ChIP) was performed in HepG2 cells (Fig. 3C). After 6 h of panobinostat treatment, binding of p53 to its responsive element (p53RE) in the p21 promoter region was observed that was followed by a transactivation of the Sp1 binding site after 24 h. These results support the western blot results showing that panobinostat increases the expression of $p21^{cip1/waf1}$ in p53-competent cells via transcriptional regulation. The transient increase in $p21^{cip1/waf1}$ protein in p53-deficient Hep3B cells is in line with the model of releasing HDAC as a transcriptional co-repressor without activation of the p53-dependent transcription process [29].

We then analysed further molecules related to HDACi growth inhibitory effects by western blot (Fig. 3D). An increase in acetylated histone H3 and H4 was observed in both cell lines. Phosphorylated H2AX, a marker for DNA double strand breaks, was strongly increased in Hep3B but showed only a modest increase in HepG2, indicating p53-dependent repair processes in this cell line. Expression of phosphorylated p38-MAPK, JNK and ERK were transiently increased in HepG2 (strongest early increase of p-p38 at 6 h, p-ERK and p-JNK highest expression at 24 h) but were completely lost after 48 h. In Hep3B, which was nearly unchanged for p-p38 and p-JNK, only p-ERK showed a slight increase at 6 h.

3.4. Panobinostat induces the unfolded protein response

As these results cannot sufficiently explain the induction of apoptosis, we investigated alternative pathways of apoptosis induction by quantitative real-time RT-PCR and western blotting. A decrease in XBP-1 mRNA (i.e., splicing of the cognate mRNA) was observed in both cell lines (0.8-fold of control in both cell lines, data not shown). The subsequent induction of mRNA of the downstream target CHOP was observed esp. in p53-competent HepG2 (2.3-fold) while CHOP-levels were stable in p53-deficient Hep3B (Fig. 4A), indicating a contribution of the unfolded protein response and endoplasmic reticulum stress in panobinostat-induced apoptosis. This was further corroborated by an activation of the ER-stress associated caspase 12 in both cell lines after 48 h (Fig. 4B). Blocking of caspase 12 by pre-incubation with ATAD significantly reduced the activity of the executioner caspases 3/7 (Fig. 4C), indicating that the activated UPR/ER-stress pathway initiates the observed cell death. The expression of associated proteins was determined by westernblotting and showed a stable expression of eIF2α, but an increase in the active phosphorylated form, esp. in Hep3B cells (Fig. 4D). Levels of CHOP protein remained stable after treatment with panobinostat indicating a differential regulation of mRNA and protein of CHOP in this setting.

3.5. Panobinostat delays growth of HCC xenografts in nude mice

HepG2 xenografts were established in male NMRI nude mice and treated with daily intraperitoneal injections of 10 mg/kg panobinostat when tumors reached a diameter of 7 mm. Panobinostat significantly delayed the growth of HCC xenografts (Fig. 5A): control tumors from mice receiving vehicle injections doubled their size in 12 days, while panobinostat treated tumors did not reach a tumor doubling in 30 days. Despite the daily injections, panobinostat was well tolerated. Transient diarrhea was observed in 3 animals from the

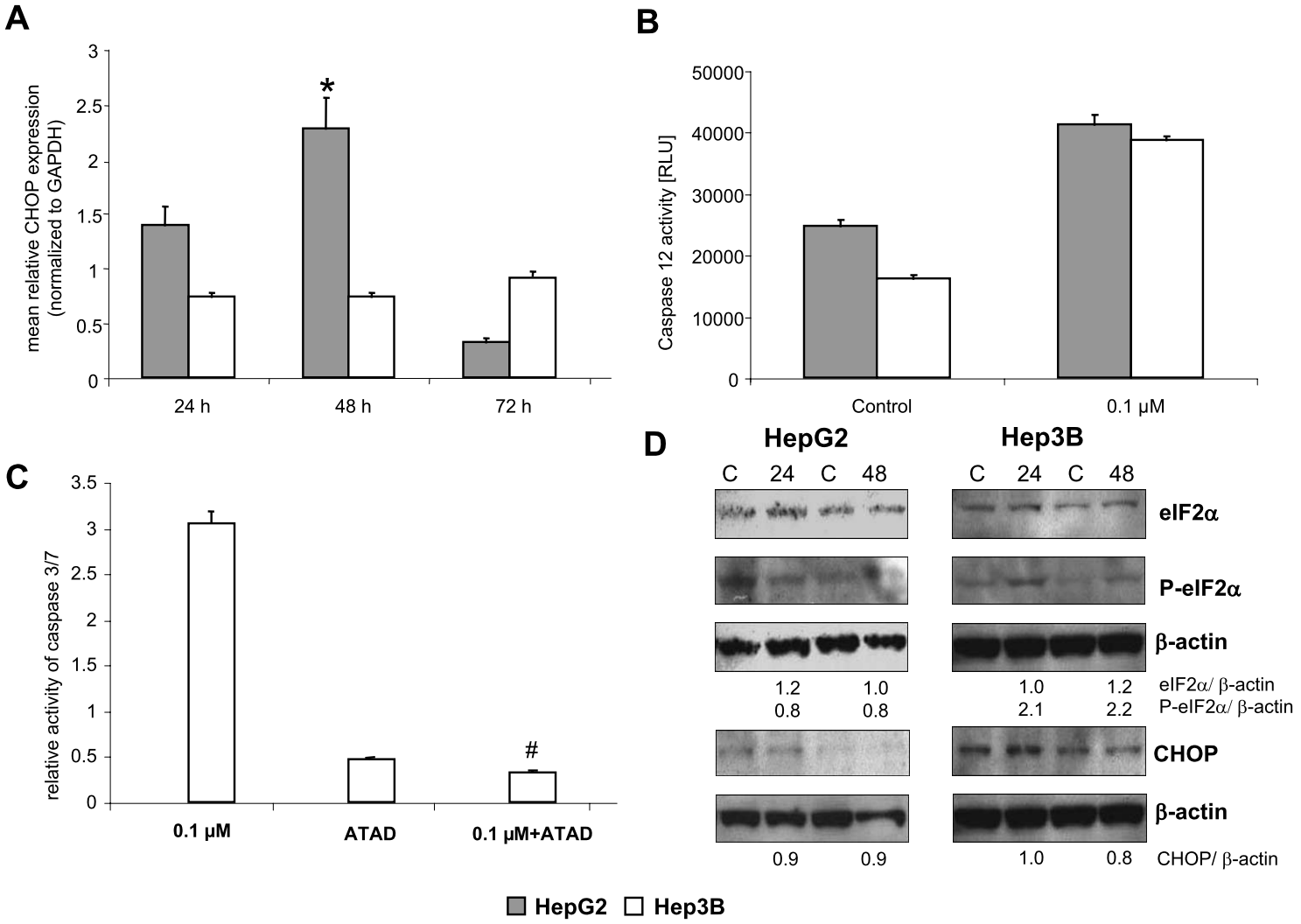

Fig. 4. Analysis of alternative apoptosis pathways. Quantitative *real-time* RT-PCR analysis of the endoplasmic reticulum stress related gene CHOP shows a significant induction of the UPR after 48 h in HepG2 but not in Hep3B (A). Results were normalized to GAPDH expression levels. Activity of the ER-stress associated caspase 12 was increased after panobinostat treatment (B). Downstream activity of caspases 3/7 was decreased after inhibition of caspase 12 with ATAD (C). Westernblot analysis of effector proteins of ER stress after 24 and 48 h treatment with 0.1 µM panobinostat (D). $^{*}P < 0.05$ vs. control or $^{\#}P < 0.05$ vs. panobinostat alone.

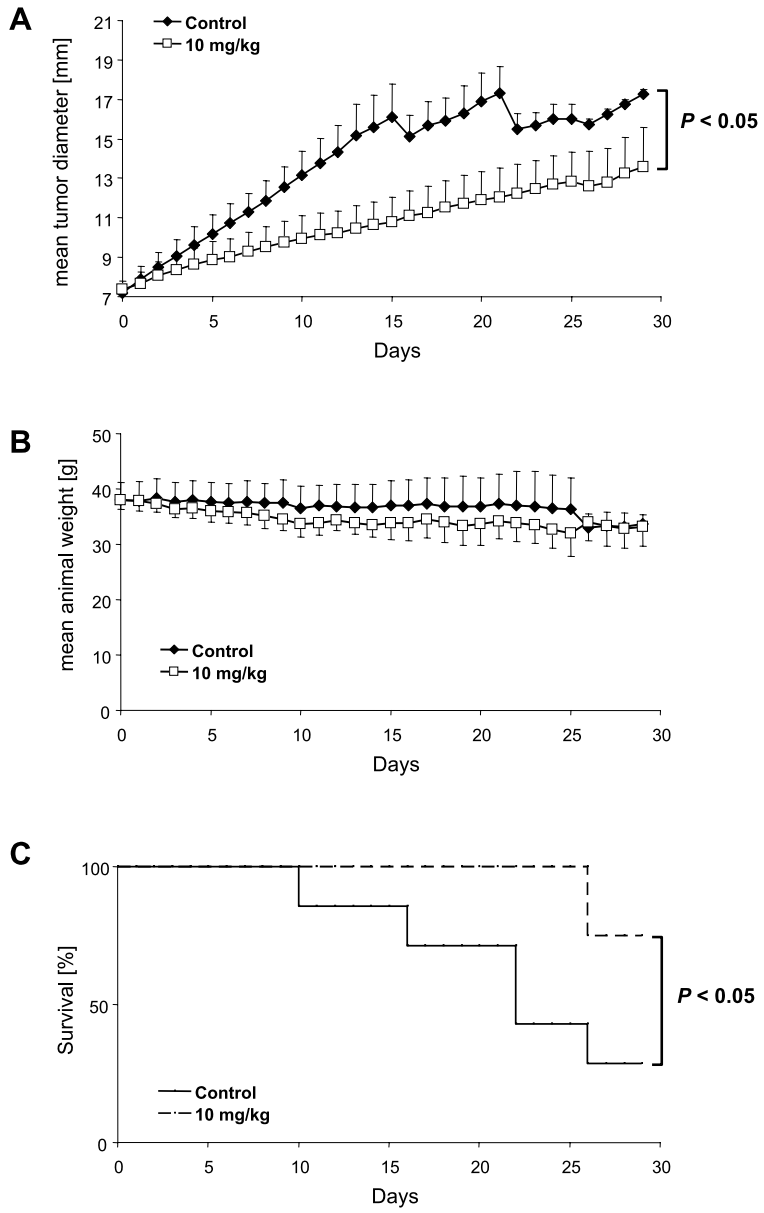

Fig. 5. Panobinostat for treatment of HepG2 xenografts in nude mice. Animals were treated with daily i.p. injections of 10 mg/kg panobinostat or vehicle control. Mean tumor size (A) and animal weight (B) ± SEM of 8 animals/group. (C) Survival analysis of 8 animals/group. All surviving animals were censored on day 30 due to animal protection rules. Mean tumor size in the control group is reduced at days 16 and 22 due to the removal of animals with a tumor diameter of more than 25 mm with respect to animal welfare regulations.

panobinostat group but animal weight remained stable during the course of the experiment (Fig. 5B). Panobinostat significantly prolonged the survival of treated animals (Fig. 5C). Mean survival time was 21 days for control mice and more than 30 days in the treated group.

Macroscopically, treated tumors showed a decreased size and vessel density (Fig. 6b, d) compared to controls (Fig. 6a, c). Normal liver histology (not shown) was unaffected without signs of toxic liver damage as determined by serum ALT levels (Fig. 6e). Immunohistochemistry revealed a decreased Ki-67 labeling index (24.8% vs. 13.9%; $P < 0.05$; Fig. 6f, g, h) that was paralleled by an increase in TUNEL positive cells (Fig. 6i, j) and an overall increase in relative necrosis area in all analyzed samples (41.7% vs. 54.6%;

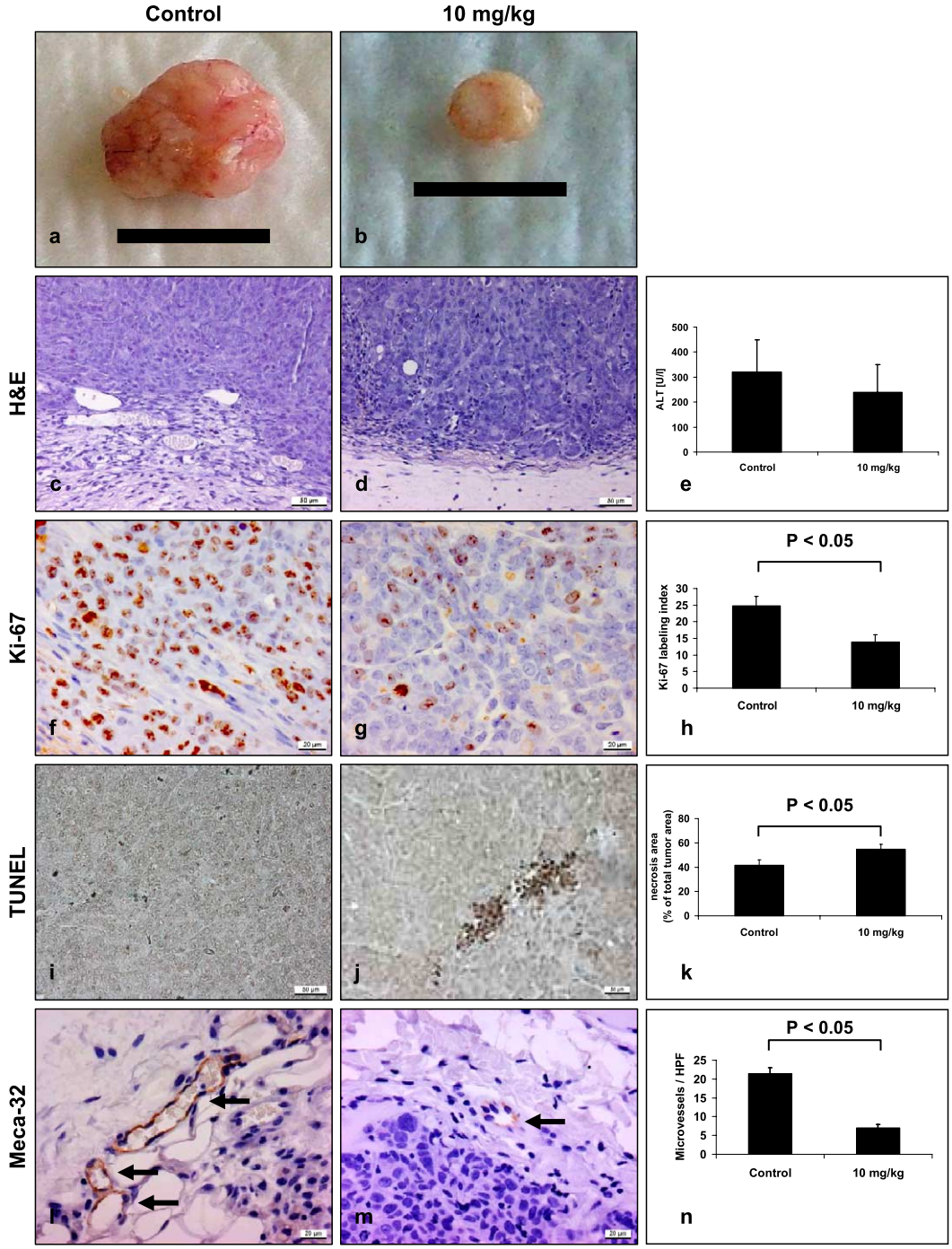

Fig. 6. Morphologic analysis of HepG2 xenografts treated with panobinostat. Representative tumors are shown from vehicle treated controls (a) or animals receiving daily i.p. injection of 10 mg/kg panobinostat for 30 days (b) and related H&E stainings (c, d). Bar in (a) and (b) is 1 cm. (e) shows mean ALT levels ± SEM of 8 animals/group. Ki-67 stainings (f, g) showed a significant reduction of the proliferation index (h) in panobinostat treated animals, paralleled by an increase in TUNEL positive cells (i, j) and total necrosis area (k). Endothelial cell stainings with the Meca-32 antibody (arrows in l and m) revealed a significantly decreased microvessel density (n) after panobinostat treatment. Results in (h), (k) and (n) are mean ± SEM of 4 independent high power fields of sections of 8 animals/group. Magnification is 200× for (c, d) and (i, j) and 400× for (f, g) and (l, m).

$P < 0.05$; Fig. 6k). Endothelial cell stainings with the Meca-32 antibody (Fig. 6l, m) showed a significant reduction of the mean microvessel density per group from 21.4 to 6.9 microvessels per high power field ($P < 0.05$; Fig. 6n).

Quantitative real-time RT-PCR from xenograft samples revealed a significant increase in expression of $p21^{cip1/waf1}$, bcl-xL, bcl-xS and the pro-apoptotic TRAIL receptor hDR4 (Fig. 7A). This pattern reflects the changes observed from HepG2 *in vitro* samples (Fig. 3B). Interestingly, HepG2 xenografts also show an increased expression of hDR4, which was not observed *in vitro*. This finding can be explained by an altered tumor environment *in vivo*, which fosters pro-apoptosis by the extrinsic pathway, too. The expression of $p21^{cip1/waf1}$ was increased by approx. 30% in the xenografts as evidenced by western blot analysis (Fig. 7B). In treated tumors, a 30% overall increase in acetylated histones H3 and H4 was observed, too.

4. Discussion

Our results show that the novel pan-DACi panobinostat (LBH589) reduces cell proliferation of human HCC cell lines, induces DNA damage and apoptotic cell death *in vitro* and in a subcutaneous xenograft model. While a contribution of the mitochondrial pathway in HDACi mediated apoptosis in HCC models has been shown previously for other compounds [12,18], the cinnamic hydroxamic acid panobinostat does not seem to exert its pro-apoptotic effect by this way as no significant changes in the bax/bcl-2 ratio or in mitochondrial integrity as determined by $DiOC_6$ staining were observed.

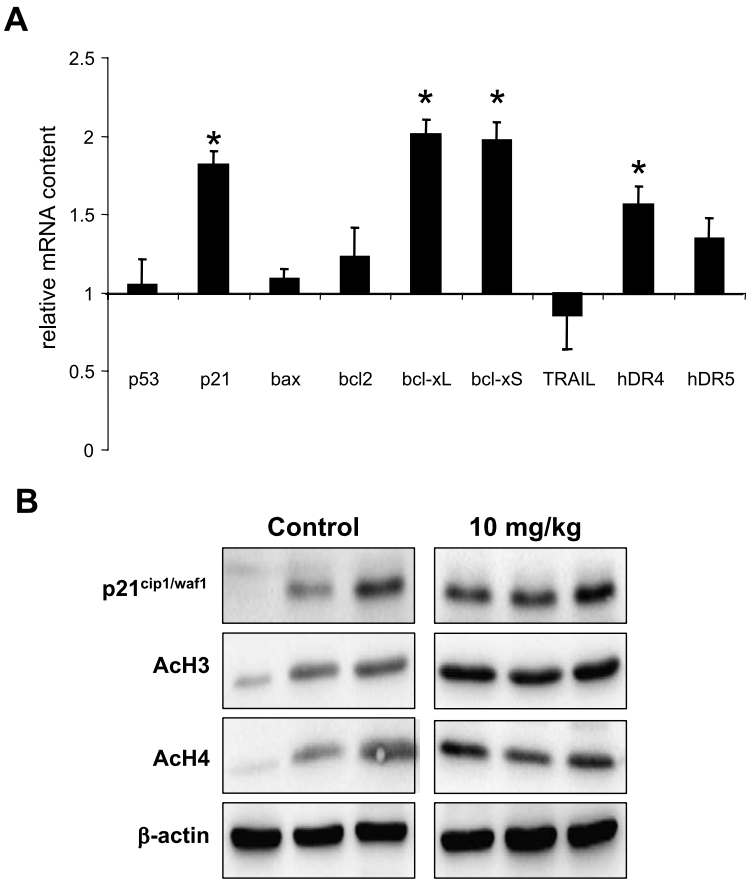

Fig. 7. Molecular analysis of panobinostat treated HepG2 xenografts. (A) Quantitative *real-time* RT-PCR analysis of panobinostat-related genes. Results were normalized to GAPDH mRNA expression and are presented as mean ± SEM of 8 animals/group relative to mRNA levels of control animals set at 1.0. $*P < 0.05$ vs. control. (B) Western blot analysis from 3 representative animals/group showing an increase in $p21^{cip1/waf1}$ and acetylated histone H3 and H4.

4.1. Panobinostat and apoptosis dependent pathways

We have shown that panobinostat induces DNA double strand breaks, probably via generation of reactive oxygen species, which was previously demonstrated for other DACi by others [45]. Only a modest increase of phosphorylated H2AX as a marker of DNA damage was found in p53-competent HepG2, indicating intact cellular DNA repair processes in this cell line. In contrast, a more than 6-fold increase in P-H2AX was found in p53-deficient Hep3B. Cellular stress has also been linked to a p53-dependent activation of the MAPK pathway, while activated MAPK themselves can phosphorylate p53 [42]. Besides ROS, the unfolded protein response (UPR) has been shown to induce JNK phosphorylation and thus lead to growth arrest and apoptosis induction via caspase 12 [31,37]. Indeed, we could demonstrate a transient activation of MAPK members and a splicing of the XBP-1 mRNA with induction of its downstream target CHOP and increased phosphorylation of eIF2α after treatment with panobinostat in. The UPR can also be induced independent of p53 by hyperacetylation and inhibition of chaperones [8,24]. The chaperone function of Hsp90 can be inhibited by DACi, including panobinostat, and may therefore contribute to this novel pathway of apoptosis induction [2,10,13,14]. Other pathways independent of p53 include an increase in NF-κB p50/p65 nuclear translocation or the activation of the RNA-dependent protein kinase which leads to phosphorylation of IκB [36]. Activation of caspase 12 has been shown to cleave pro-caspase 9 without disturbing mitochondrial integrity after UPR and ER stress induction, which is in line with the results shown here [21,35]. It has to be stated, however, that the role of caspase 12 is still under debate in human cells, as contradicting data have been reported on the existence of caspase 12 in humans or if splice variants of this gene locus, which also encodes for caspase 1, 4 and 5, are related to the observed phenomena [22,25]. Further studies are therefore needed to clarify the role of caspase 12 and UPR-related pathways after DACi in HCC.

Previous results from our group and from others have shown that DACi induce apoptosis also via the extrinsic pathway with a preference of the death receptors hDR4 or hDR5 [32,47]. Interestingly, we also found a strong activation of the extrinsic initiator caspase 8 in p53-deficient Hep3B cells, paralleled by an increase in hDR4 mRNA levels in this cell line, although this pathway does not seem to contribute functionally to apoptosis induction as was shown by blocking hDR4 with specific antibodies. Yet, the upregulation of the death receptor and the strong induction of caspase 8 points to a sensitizing effect of extrinsic apoptosis inducers by DACi [5,32,47].

Recently, inhibition of HDAC7 by panobinostat has been shown to induce the expression and translocation of the orphan nuclear receptor Nur77 in human cutaneous T-cell lymphoma cell lines which leads to interference with the mitochondrial apoptosis cascade [7]. In HCC, the expression of HDAC7 has not yet been investigated and the contribution of this pathways in relation the p53 status is also unknown yet. Interestingly, the inhibition of HDAC7 has been closely related to the anti-angiogenic effect of HDACi which may explain the observed decrease in microvessel density in our model [6,26].

4.2. Panobinostat and anti-proliferative effects

The anti-proliferative effects of DACi have been linked to the over-expression of $p21^{cip1/waf1}$ in human tumors including HCC [29,41]. While this effect has been demonstrated for panobinostat in different human cancers [4,23,45], we have shown for the first time a direct transcriptional regulation of $p21^{cip1/waf1}$ by panobinostat in a p53-dependent manner. Additionally, activation of the UPR has also been shown to induce a p53-dependent cell cycle arrest via transcriptional regulation of $p21^{cip1/waf1}$, which can therefore contribute to the observed effects on $p21^{cip1/waf1}$ expression in HepG2 cells [46]. Yet, post-transcriptional regulatory processes independent of p53 can induce short-term expression of $p21^{cip1/waf1}$ by mRNA stabilization [19] or by release of HDAC1 from its Sp1 site which abolishes the transcriptional suppression without direct transcriptional activation [29]. This view is in concordance with the transient increase in $p21^{cip1/waf1}$ protein after 6 h of panobinostat treatment in Hep3B. Finally, $p21^{cip1/waf1}$ leads to reduced proliferation by inhibiting cell cycle progression at the G_1-phase, which was demonstrated by trypan blue staining and FACS analysis *in vitro* in both cell lines and a significantly reduced Ki-67 labeling index in the xenograft model. For panobinostat, a direct cytotoxic effect on endothelial cells has previously been described [34] and we also observed a reduced vascularization of HepG2 xenografts. These two independent pathways, presumably together with other DACi targets like MAPK and Hif-1α [44], cooperate to reduce tumor viability and may explain the good *in vivo* tolerability of DACi.

4.3. Panobinostat and antitumoral networking: Possible pathways

Based on these findings, we propose a signaling network for the antitumoral effects of panobinostat in HCC models (Fig. 8). The inhibition of different HDAC subtypes leads to increased acetylation of histones H3 and H4 which might serve as a biomarker for *in vivo* monitoring of HDACi efficacy [40]. Dependent on the p53 status, pro-apoptotic TRAIL receptors (hDR4, hDR5) are induced. Hyperacetylation of chaperones, e.g. Hsp90 and other so far unidentified proteins, activates the UPR and endoplasmic reticulum stress which interferes with the MAPK cascade (p38, ERK) and via splicing of XBP-1 and transcriptional activation of CHOP with JNK and caspase 12. Active caspase 12 can then activate the executioner caspase 3 which is also capable of activating other upstream caspases like caspase 8 [3]. MAPK and JNK can directly reduce cell proliferation by inhibiting intracellular survival signaling pathways. The increased expression of the cell cycle regulator $p21^{cip1/waf1}$ is under transcriptional control of p53 and inhibits cell cycle progression after DACi treatment. p53 also interferes with pro-angiogenic pathways, which are dependent on MAPK signaling.

DACi have been shown to generate reactive oxygen species (ROS) [16], which then leads DNA double-strand breaks as evidenced here by an increase in P-H2AX, esp. in p53-deficient Hep3B cells. P-H2AX itself is capable of inducing p53-dependent DNA repair processes [20,33] as we demonstrated by a reduced expression of this marker in HepG2 cells compared to Hep3B. These findings, together with the low response of apoptosis induction in HF cells, show that non-transformed p53wt cells may be protected from undesired treatment effects of panobinostat and explain the good tolerability of this compound *in vivo*.

In summary, our results show that the novel pan-DACi panobinostat effectively suppresses growth sig-

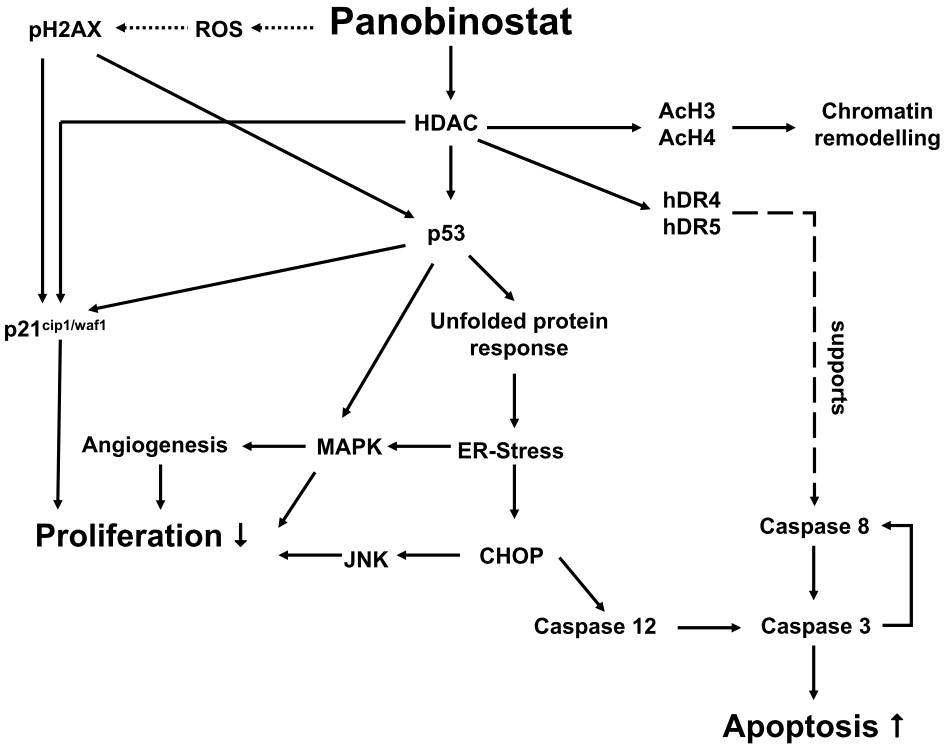

Fig. 8. Signaling pathways involved in panobinostat mediated anti-cancer activity in hepatocellular carcinoma. The inhibition of HDAC by panobinostat leads to an increase in acetylated histones H3 and H4 indicating the chromatin remodeling properties of panobinostat. Dependent on the p53 status, several pro-apoptotic (e.g., TRAIL receptor system, unfolded protein response) and anti-proliferative pathways (e.g., $p21^{cip1/waf1}$) are activated. Additional effects included the generation of DNA double-strand breaks (pH2AX) and the inhibition of MAPK pathways. These factors also inhibit tumor related neo-angiogenesis and lead to reduced growth of xenografts. The dotted line depicts the generation of reactive oxygen species (ROS) as evidenced in the literature for other HDACi. The increased expression of death receptors (hDR4 or hDR5) may enhance the effect of caspase 8 but is not mechanistically linked to caspase 8 activation (dashed line).

naling pathways in human HCC models and induces alternative apoptotic pathways dependent on the p53 status. It is important to note that panobinostat exerts pro-apoptotic effects also in p53 negative cells, which implicates a broad applicability in human tumors. As inhibition of MAPK signaling has recently been established as the first-line treatment of advanced HCC [1], combination approaches with sorafenib and panobinostat are urgently warranted to improve the treatment options for HCC.

Acknowledgements

We are indebted to Gabriele Krumholz for support in animal care and experiments. The excellent technical assistance of Astrid Taut, Isabel Zeitträger and Ines Grob-Achleitner is gratefully acknowledged. The study was supported by a grant from Novartis Pharma GmbH, Germany, to M. Ocker, the ELAN programme of the University Hospital Erlangen (07.09.24.1) and a fellowship of the European Association for the Study of the Liver (EASL) to P. Di Fazio and a grant of the Wilhelm-Sander-Foundation (2005.031.2).

References

[1] G.K. Abou-Alfa, L. Schwartz, S. Ricci, D. Amadori, A. Santoro, A. Figer, J. De Greve, J.Y. Douillard, C. Lathia, B. Schwartz, I. Taylor, M. Moscovici and L.B. Saltz, Phase II study of sorafenib in patients with advanced hepatocellular carcinoma, *J. Clin. Oncol.* **24** (2006), 4293–4300.

[2] P. Bali, M. Pranpat, J. Bradner, M. Balasis, W. Fiskus, F. Guo, K. Rocha, S. Kumaraswamy, S. Boyapalle, P. Atadja, E. Seto and K. Bhalla, Inhibition of histone deacetylase 6 acetylates and disrupts the chaperone function of heat shock protein 90: a novel basis for antileukemia activity of histone deacetylase inhibitors, *J. Biol. Chem.* **280** (2005), 26729–26734.

[3] R.C. Bleackley and J.A. Heibein, Enzymatic control of apoptosis, *Nat. Prod. Rep.* **18** (2001), 431–440.

[4] T. Bluethner, M. Niederhagen, K. Caca, F. Serr, H. Witzigmann, C. Moebius, J. Mossner and M. Wiedmann, Inhibition of histone deacetylase for the treatment of biliary tract cancer: a new effective pharmacological approach, *World J. Gastroenterol.* **13** (2007), 4761–4770.

[5] L.M. Butler, V. Liapis, S. Bouralexis, K. Welldon, S. Hay, M. Thai le, A. Labrinidis, W.D. Tilley, D.M. Findlay and A. Evdokiou, The histone deacetylase inhibitor, suberoylanilide hydroxamic acid, overcomes resistance of human breast cancer cells to Apo2L/TRAIL, *Int. J. Cancer* **119** (2006), 944–954.

[6] S. Chang, B.D. Young, S. Li, X. Qi, J.A. Richardson and E.N. Olson, Histone deacetylase 7 maintains vascular integrity by repressing matrix metalloproteinase 10, *Cell* **126** (2006), 321–334.

[7] J. Chen, W. Fiskus, K. Eaton, P. Fernandez, Y. Wang, R. Rao, P. Lee, R. Joshi, Y. Yang, R. Kolhe, R. Balusu, P. Chappa, K. Natarajan, A. Jillella, P. Atadja and K.N. Bhalla, Co-treatment with BCL-2 antagonist sensitizes cutaneous T cell lymphoma to lethal action of HDAC7-Nur77 based mechanism, *Blood* **113** (2009), 4038–4048.

[8] E.L. Davenport, H.E. Moore, A.S. Dunlop, S.Y. Sharp, P. Workman, G.J. Morgan and F.E. Davies, Heat shock protein inhibition is associated with activation of the unfolded protein response pathway in myeloma plasma cells, *Blood* **110** (2007), 2641–2649.

[9] M. Duvic and J. Vu, Vorinostat: a new oral histone deacetylase inhibitor approved for cutaneous T-cell lymphoma, *Expert Opin. Investig. Drugs* **16** (2007), 1111–1120.

[10] A. Edwards, J. Li, P. Atadja, K. Bhalla and E.B. Haura, Effect of the histone deacetylase inhibitor LBH589 against epidermal growth factor receptor-dependent human lung cancer cells, *Mol. Cancer Ther.* **6** (2007), 2515–2524.

[11] H.B. El-Serag and K.L. Rudolph, Hepatocellular carcinoma: epidemiology and molecular carcinogenesis, *Gastroenterology* **132** (2007), 2557–2576.

[12] S. Emanuele, M. Lauricella, D. Carlisi, B. Vassallo, A. D'Anneo, P. Di Fazio, R. Vento and G. Tesoriere, SAHA induces apoptosis in hepatoma cells and synergistically interacts with the proteasome inhibitor Bortezomib, *Apoptosis* **12** (2007), 1327–1338.

[13] W. Fiskus, Y. Ren, A. Mohapatra, P. Bali, A. Mandawat, R. Rao, B. Herger, Y. Yang, P. Atadja, J. Wu and K. Bhalla, Hydroxamic acid analogue histone deacetylase inhibitors attenuate estrogen receptor-alpha levels and transcriptional activity: a result of hyperacetylation and inhibition of chaperone function of heat shock protein 90, *Clin. Cancer Res.* **13** (2007), 4882–4890.

[14] P. George, P. Bali, S. Annavarapu, A. Scuto, W. Fiskus, F. Guo, C. Sigua, G. Sondarva, L. Moscinski, P. Atadja and K. Bhalla, Combination of the histone deacetylase inhibitor LBH589 and the hsp90 inhibitor 17-AAG is highly active against human CML-BC cells and AML cells with activating mutation of FLT-3, *Blood* **105** (2005), 1768–1776.

[15] F. Giles, T. Fischer, J. Cortes, G. Garcia-Manero, J. Beck, F. Ravandi, E. Masson, P. Rae, G. Laird, S. Sharma, H. Kantarjian, M. Dugan, M. Albitar and K. Bhalla, A phase I study of intravenous LBH589, a novel cinnamic hydroxamic acid analogue histone deacetylase inhibitor, in patients with refractory hematologic malignancies, *Clin. Cancer Res.* **12** (2006), 4628–4635.

[16] C. Habold, A. Poehlmann, K. Bajbouj, R. Hartig, K.S. Korkmaz, A. Roessner and R. Schneider-Stock, Trichostatin A causes p53 to switch oxidative-damaged colorectal cancer cells from cell cycle arrest into apoptosis, *J. Cell. Mol. Med.* **12** (2008), 607–621.

[17] R. Hallmann, D.N. Mayer, E.L. Berg, R. Broermann and E.C. Butcher, Novel mouse endothelial cell surface marker is suppressed during differentiation of the blood brain barrier, *Dev. Dyn.* **202** (1995), 325–332.

[18] C. Herold, M. Ganslmayer, M. Ocker, M. Hermann, A. Geerts, E.G. Hahn and D. Schuppan, The histone-deacetylase inhibitor Trichostatin A blocks proliferation and triggers apoptotic programs in hepatoma cells, *J. Hepatol.* **36** (2002), 233–240.

[19] C.L. Hirsch and K. Bonham, Histone deacetylase inhibitors regulate p21WAF1 gene expression at the post-transcriptional level in HepG2 cells, *FEBS Lett.* **570** (2004), 37–40.
[20] K.K. Khanna and S.P. Jackson, DNA double-strand breaks: signaling, repair and the cancer connection, *Nat. Genet.* **27** (2001), 247–254.
[21] R. Kim, M. Emi, K. Tanabe and S. Murakami, Role of the unfolded protein response in cell death, *Apoptosis* **11** (2006), 5–13.
[22] M. Lamkanfi, N. Festjens, W. Declercq, T. Vanden Berghe and P. Vandenabeele, Caspases in cell survival, proliferation and differentiation, *Cell Death Differ.* **14** (2007), 44–55.
[23] P. Maiso, X. Carvajal-Vergara, E.M. Ocio, R. Lopez-Perez, G. Mateo, N. Gutierrez, P. Atadja, A. Pandiella and J.F. San Miguel, The histone deacetylase inhibitor LBH589 is a potent antimyeloma agent that overcomes drug resistance, *Cancer Res.* **66** (2006), 5781–5789.
[24] M.G. Marcu, M. Doyle, A. Bertolotti, D. Ron, L. Hendershot and L. Neckers, Heat shock protein 90 modulates the unfolded protein response by stabilizing IRE1alpha, *Mol. Cell. Biol.* **22** (2002), 8506–8513.
[25] T. Momoi, Caspases involved in ER stress-mediated cell death, *J. Chem. Neuroanat.* **28** (2004), 101–105.
[26] D. Mottet, A. Bellahcene, S. Pirotte, D. Waltregny, C. Deroanne, V. Lamour, R. Lidereau and V. Castronovo, Histone deacetylase 7 silencing alters endothelial cell migration, a key step in angiogenesis, *Circ. Res.* **101** (2007), 1237–1246.
[27] D. Neureiter, S. Zopf, T. Leu, O. Dietze, C. Hauser-Kronberger, E.G. Hahn, C. Herold and M. Ocker, Apoptosis, proliferation and differentiation patterns are influenced by Zebularine and SAHA in pancreatic cancer models, *Scand. J. Gastroenterol.* **42** (2007), 103–116.
[28] M. Ocker, A. Alajati, M. Ganslmayer, S. Zopf, M. Luders, D. Neureiter, E.G. Hahn, D. Schuppan and C. Herold, The histone-deacetylase inhibitor SAHA potentiates proapoptotic effects of 5-fluorouracil and irinotecan in hepatoma cells, *J. Cancer Res. Clin. Oncol.* **131** (2005), 385–394.
[29] M. Ocker and R. Schneider-Stock, Histone deacetylase inhibitors: signalling towards p21cip1/waf1, *Int. J. Biochem. Cell Biol.* **39** (2007), 1367–1374.
[30] K. Okamoto, D. Neureiter and M. Ocker, Biomarkers for novel targeted therapies of hepatocellular carcinoma, *Histol. Histopathol.* **24** (2009), 493–502.
[31] S. Oyadomari and M. Mori, Roles of CHOP/GADD153 in endoplasmic reticulum stress, *Cell Death Differ.* **11** (2004), 381–389.
[32] A. Pathil, S. Armeanu, S. Venturelli, P. Mascagni, T.S. Weiss, M. Gregor, U.M. Lauer and M. Bitzer, HDAC inhibitor treatment of hepatoma cells induces both TRAIL-independent apoptosis and restoration of sensitivity to TRAIL, *Hepatology* **43** (2006), 425–434.
[33] T.T. Paull, E.P. Rogakou, V. Yamazaki, C.U. Kirchgessner, M. Gellert and W.M. Bonner, A critical role for histone H2AX in recruitment of repair factors to nuclear foci after DNA damage, *Curr. Biol.* **10** (2000), 886–895.
[34] D.Z. Qian, Y. Kato, S. Shabbeer, Y. Wei, H.M. Verheul, B. Salumbides, T. Sanni, P. Atadja and R. Pili, Targeting tumor angiogenesis with histone deacetylase inhibitors: the hydroxamic acid derivative LBH589, *Clin. Cancer Res.* **12** (2006), 634–642.
[35] R.V. Rao, S. Castro-Obregon, H. Frankowski, M. Schuler, V. Stoka, G. del Rio, D.E. Bredesen and H.M. Ellerby, Coupling endoplasmic reticulum stress to the cell death program. An Apaf-1-independent intrinsic pathway, *J. Biol. Chem.* **277** (2002), 21836–21842.
[36] M.A. Robbins, L. Maksumova, E. Pocock and J.K. Chantler, Nuclear factor-kappaB translocation mediates double-stranded ribonucleic acid-induced NIT-1 beta-cell apoptosis and up-regulates caspase-12 and tumor necrosis factor receptor-associated ligand (TRAIL), *Endocrinology* **144** (2003), 4616–4625.
[37] D. Ron and P. Walter, Signal integration in the endoplasmic reticulum unfolded protein response, *Nat. Rev. Mol. Cell Biol.* **8** (2007), 519–529.
[38] R. Schneider-Stock and M. Ocker, Epigenetic therapy in cancer: molecular background and clinical development of histone deacetylase and DNA methyltransferase inhibitors, *IDrugs* **10** (2007), 557–561.
[39] M. Schwartz, S. Roayaie and M. Konstadoulakis, Strategies for the management of hepatocellular carcinoma, *Nat. Clin. Pract. Oncol.* **4** (2007), 424–432.
[40] R.P. Sharma, C. Rosen, S. Kartan, A. Guidotti, E. Costa, D.R. Grayson and K. Chase, Valproic acid and chromatin remodeling in schizophrenia and bipolar disorder: preliminary results from a clinical population, *Schizophr. Res.* **88** (2006), 227–231.
[41] I. Svechnikova, O. Ammerpohl and T.J. Ekstrom, p21waf1/Cip1 partially mediates apoptosis in hepatocellular carcinoma cells, *Biochem. Biophys. Res. Commun.* **354** (2007), 466–471.
[42] G.S. Wu, The functional interactions between the p53 and MAPK signaling pathways, *Cancer Biol. Ther.* **3** (2004), 156–161.
[43] W.S. Xu, R.B. Parmigiani and P.A. Marks, Histone deacetylase inhibitors: molecular mechanisms of action, *Oncogene* **26** (2007), 5541–5552.
[44] Q.C. Yang, B.F. Zeng, Z.M. Shi, Y. Dong, Z.M. Jiang, J. Huang, Y.M. Lv, C.X. Yang and Y.W. Liu, Inhibition of hypoxia-induced angiogenesis by trichostatin A via suppression of HIF-1a activity in human osteosarcoma, *J. Exp. Clin. Cancer Res.* **25** (2006), 593–599.
[45] C. Yu, B.B. Friday, J.P. Lai, A. McCollum, P. Atadja, L.R. Roberts and A.A. Adjei, Abrogation of MAPK and Akt signaling by AEE788 synergistically potentiates histone deacetylase inhibitor-induced apoptosis through reactive oxygen species generation, *Clin. Cancer Res.* **13** (2007), 1140–1148.
[46] F. Zhang, R.B. Hamanaka, E. Bobrovnikova-Marjon, J.D. Gordan, M.S. Dai, H. Lu, M.C. Simon and J.A. Diehl, Ribosomal stress couples the unfolded protein response to p53-dependent cell cycle arrest, *J. Biol. Chem.* **281** (2006), 30036–30045.
[47] S. Zopf, D. Neureiter, S. Bouralexis, T. Abt, K.B. Glaser, K. Okamoto, M. Ganslmayer, E.G. Hahn, C. Herold and M. Ocker, Differential response of p53 and p21 on HDAC inhibitor-mediated apoptosis in HCT116 colon cancer cells *in vitro* and *in vivo*, *Int. J. Oncol.* **31** (2007), 1391–1402.